Targeting USP7 identifies a metastasis-competent state within bone marrow-resident melanoma circulating tumor cells

Monika Vishnoi[1], Debasish Boral[1], Haowen Liu[1], Marc L. Sprouse[1], Wei Yin[1], Debalina Goswami-Sewell[1], Michael T. Tetzlaff[2], Michael A. Davies[2], Isabella C. Glitza Oliva[2], and Dario Marchetti[1]

[1]Biomarker Research Program Center, Houston Methodist Research Institute, Houston, TX

[2]Department of Melanoma Medical Oncology, The University of Texas MD Anderson Cancer Center, Houston, TX

Running Title: Molecular insights of BM-resident melanoma cells

Supplementary Information

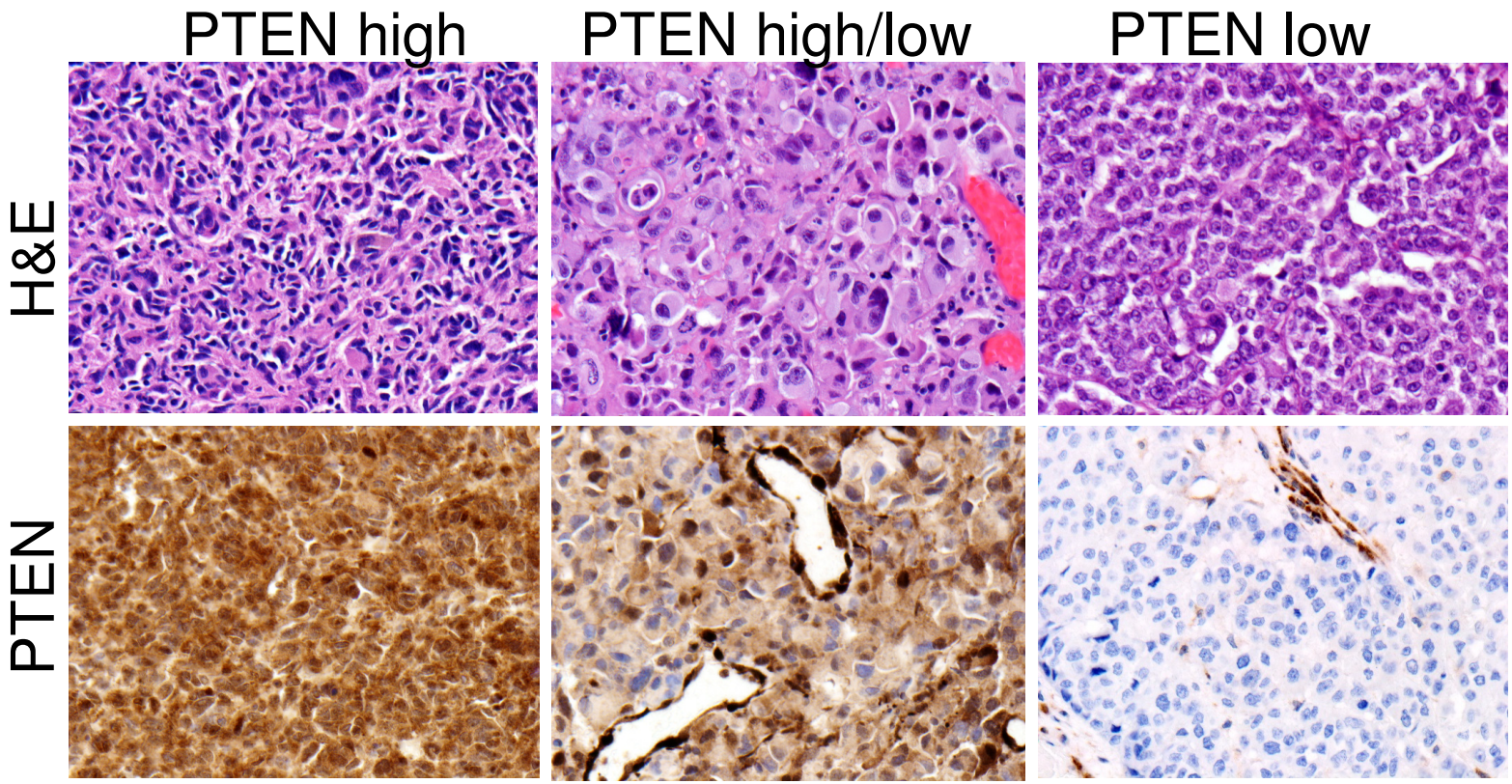

Supplementary figure S1: Melanoma patient-derived metastatic tissue (lung and liver) showing representative images of PTEN staining (200x resolution).

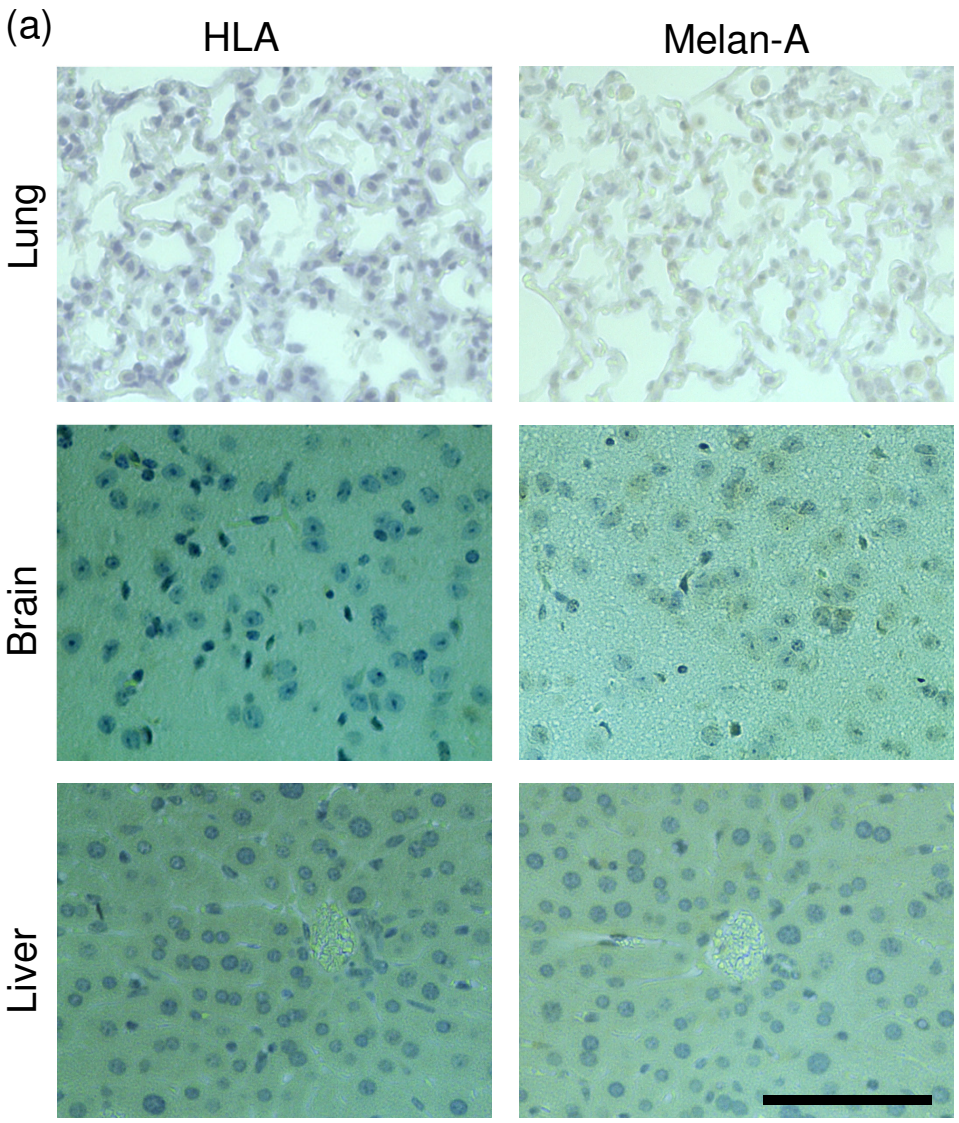

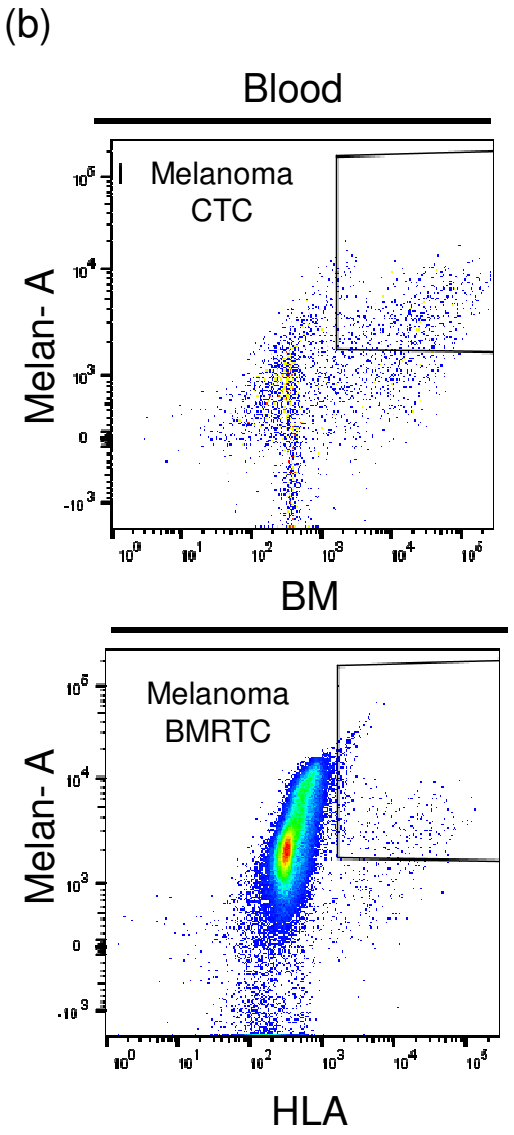

Supplementary figure S2:
Evaluation of HLA+/Melan-A+ population in different organs of CDX mice, euthanized after 3 months of Lin-neg/CTCs enriched population. (a) Immunohistochemistry analysis of HLA+ and Melan-A staining showing absence of micro-metastasis in lung, brain and liver region (scale bar=100 µM) (b) Flow-sorting analyses showing presence of HLA+/Melan-A+ population in blood and BM.

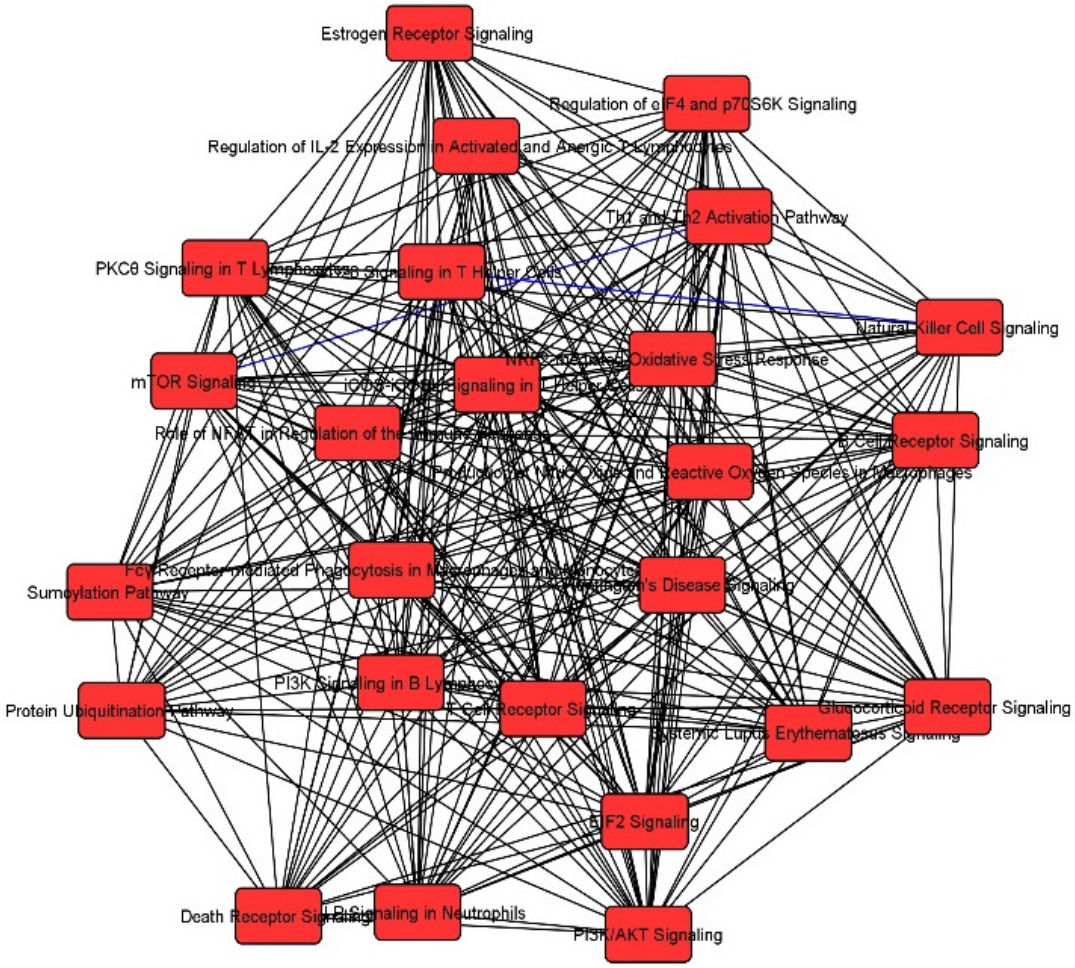

Supplementary figure S3: Molecular characterization of Lin-neg/CTC-enriched population (*de novo CTCs*). Overlapping canonical pathways in Lin-neg/CTC-enriched population by Ingenuity pathway analysis.

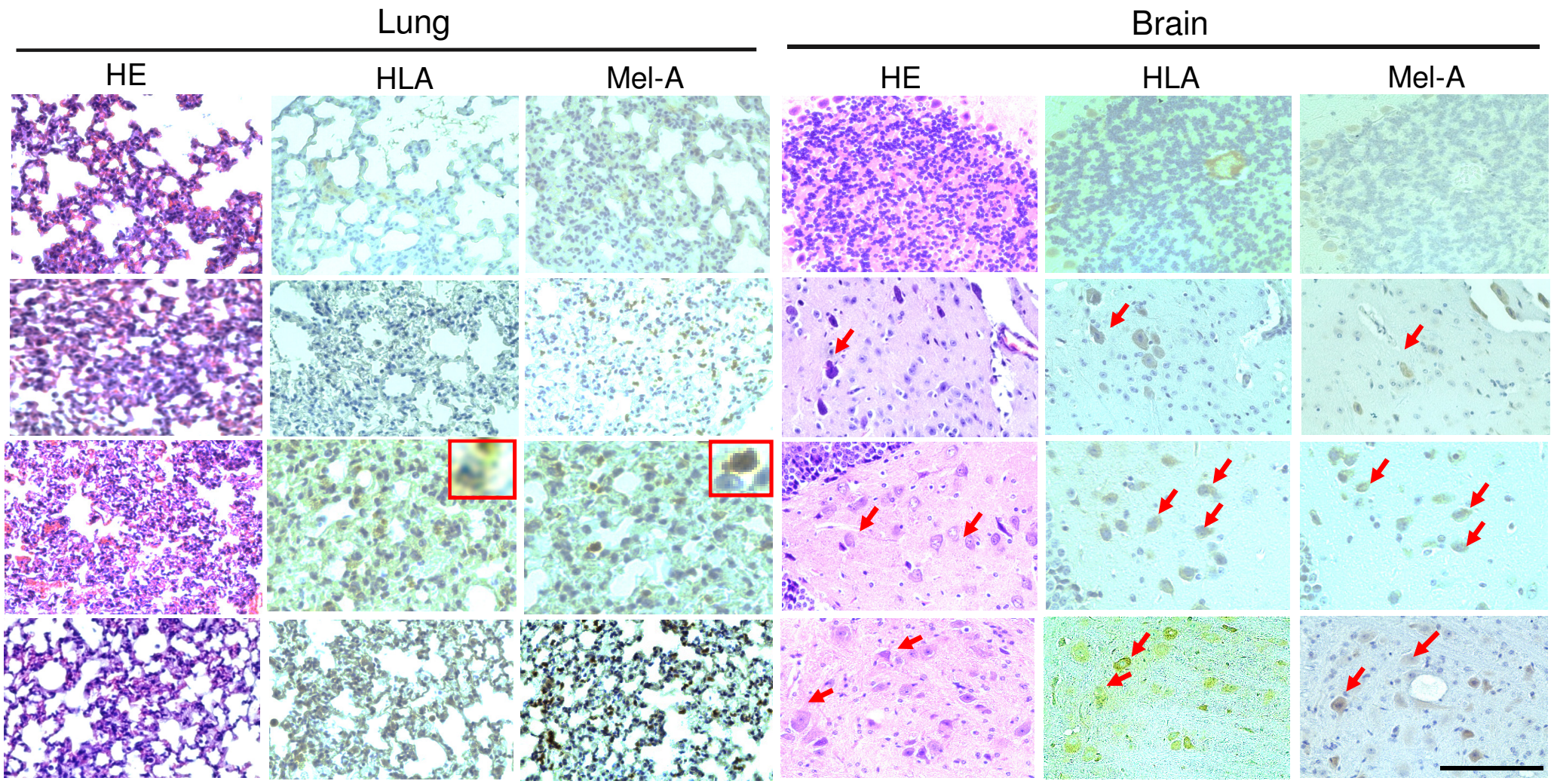

Supplementary figure S4a: Histopathological evaluation of murine xenograft tissues following CTC injection. Immunohistochemical analyses were performed to validate expression of Human-HLA-ABC and Melan-A markers in harvested xenograft lung and brain tissues. Inset and red arrows indicate representative examples of residual positive cells of respective marker staining. Brightness and contrast were adjusted for publication purposes. Scale bar=100 µM.

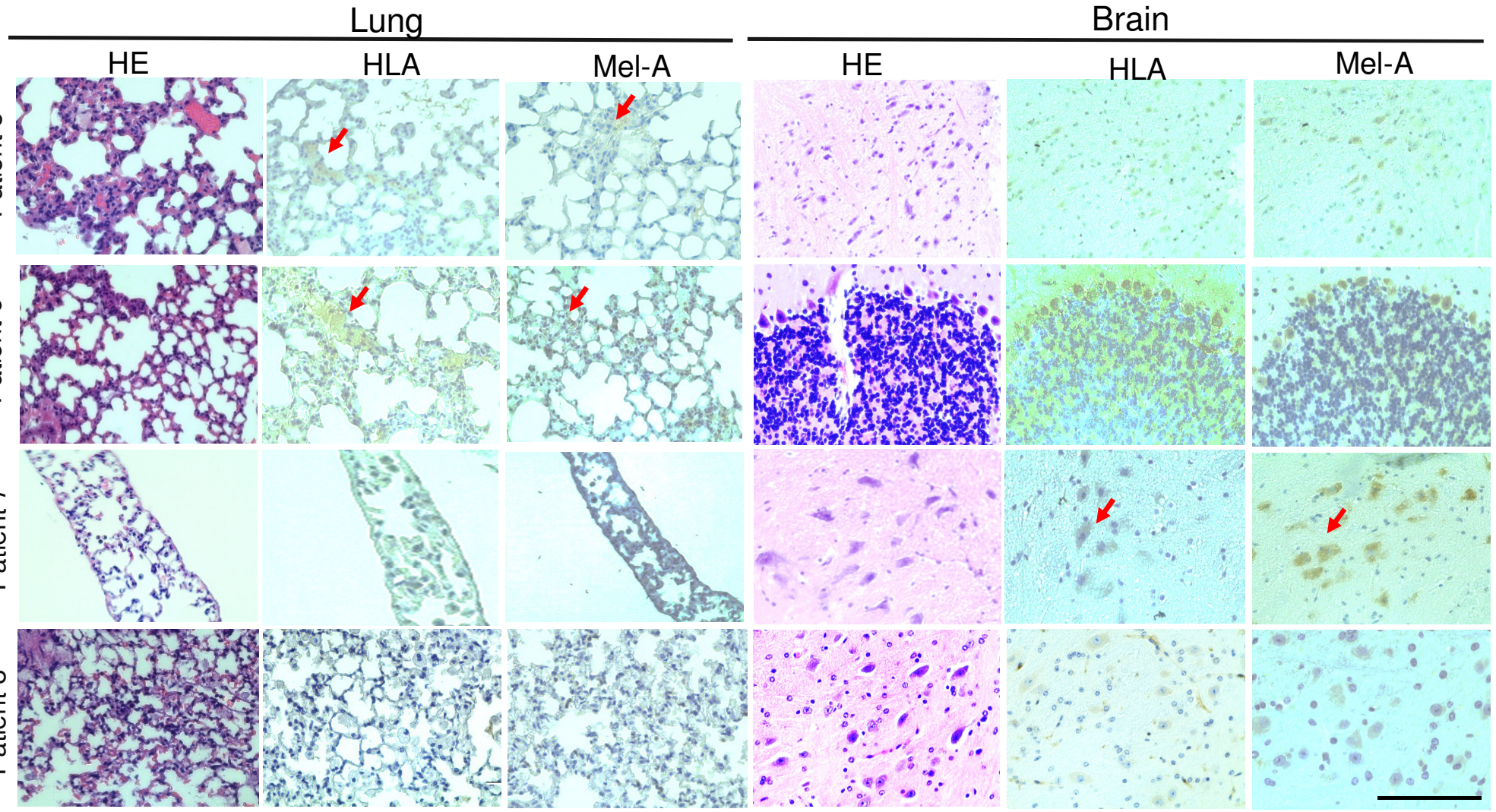

Supplementary figure S4b: Histopathological evaluation of murine xenograft tissues following CTC injection. Immunohistochemical analyses were performed to validate expression of Human-HLA-ABC and Melan-A markers in harvested xenograft lung and brain tissues. Arrows indicate representative examples of residual positive cells. Brightness and contrast were adjusted for publication purposes. Scale bar=100 µM.

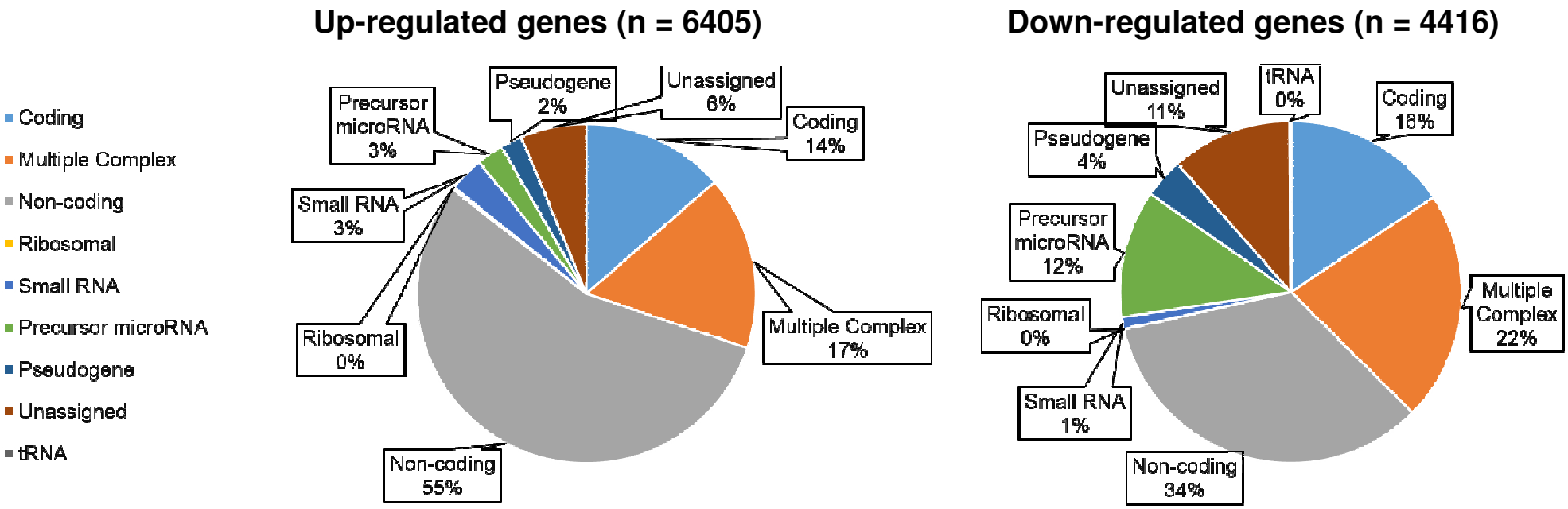

Supplementary figure S5: Transcriptome profiling of *ex vivo* vs *de novo CTCs* (Lin-neg/CTCs-enriched population) from paired patient samples (n=4). Differential gene expression analysis (Patients #2, 3, 4 and 7) showing altered up-regulated and down-regulated genes (FC=2.5; *P*-value=0.05).

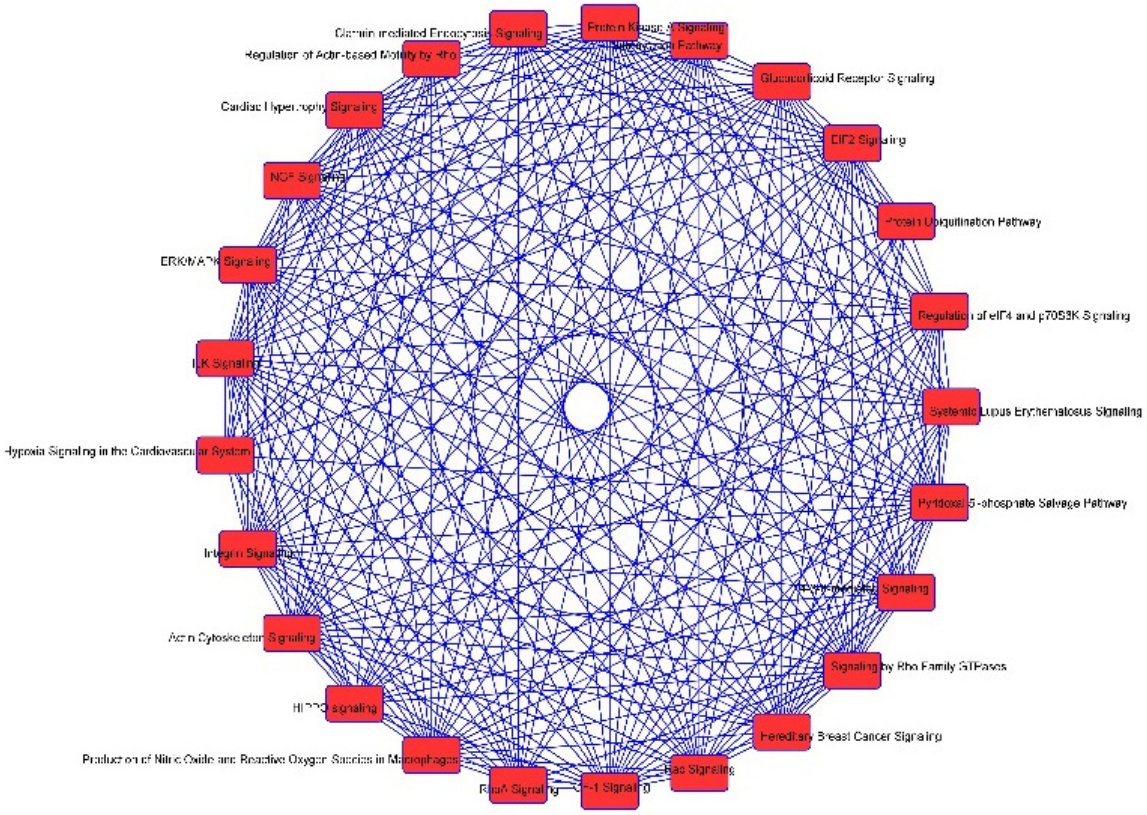

Supplementary figure S6: Transcriptome profiling of CDX BMRTCs vs. CTCs. Overlapping pathways showing altered canonical pathways in *ex-vivo* BMRTCs vs. CTCs population through Ingenuity pathway analysis.

Supplementary figure S7

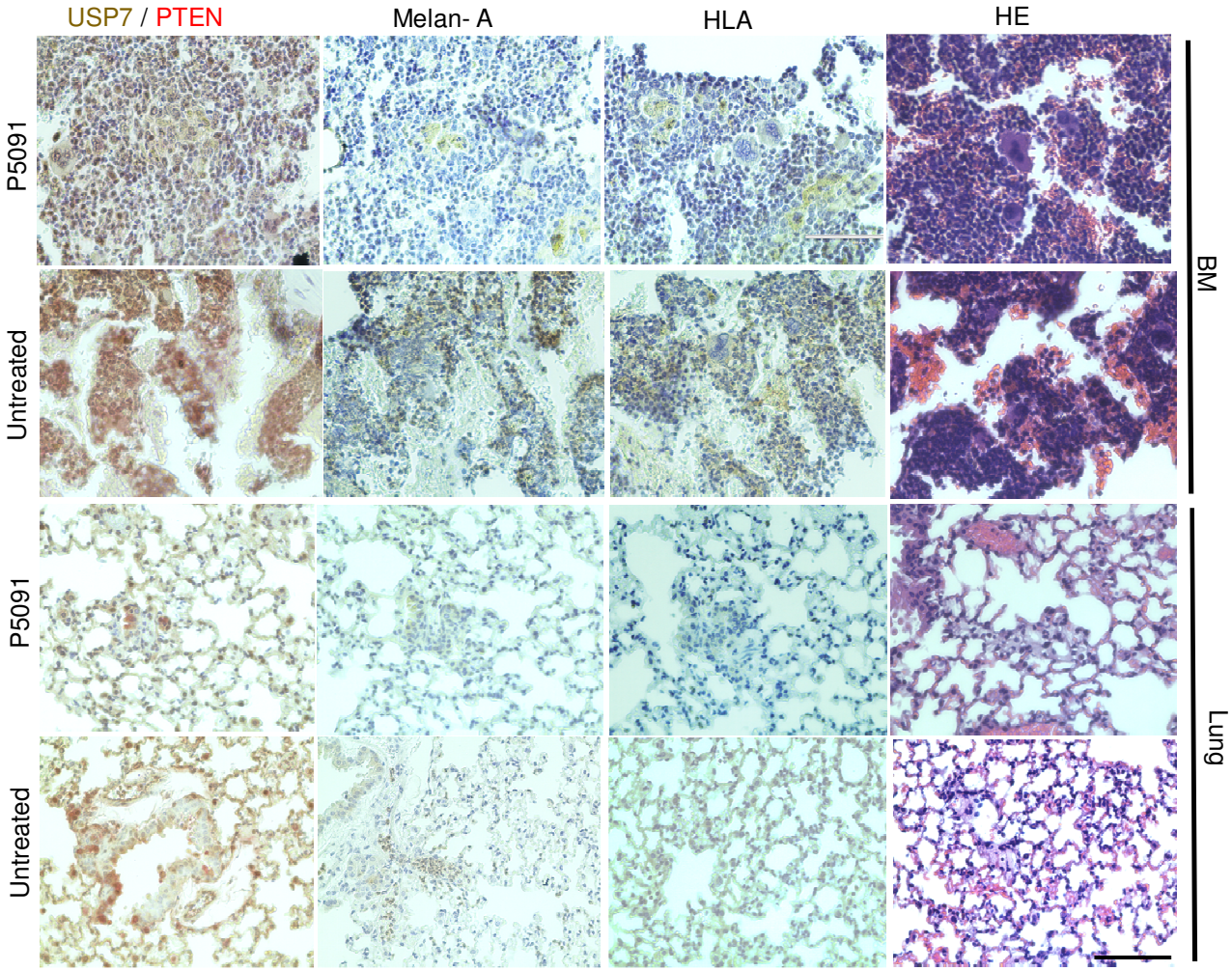

Extended figure S7a: Effect of USP7 inhibitors, P5091 on metastatic potency of BMRTCs population in CDXs. Histopathological evaluation of HLA, Melan-A, HE stain with co-localization USP7 and PTEN in similar BM and lung region derived from USP7 inhibitor treated vs. untreated from CDXs (Patient #11). Scale bar=100 µm.

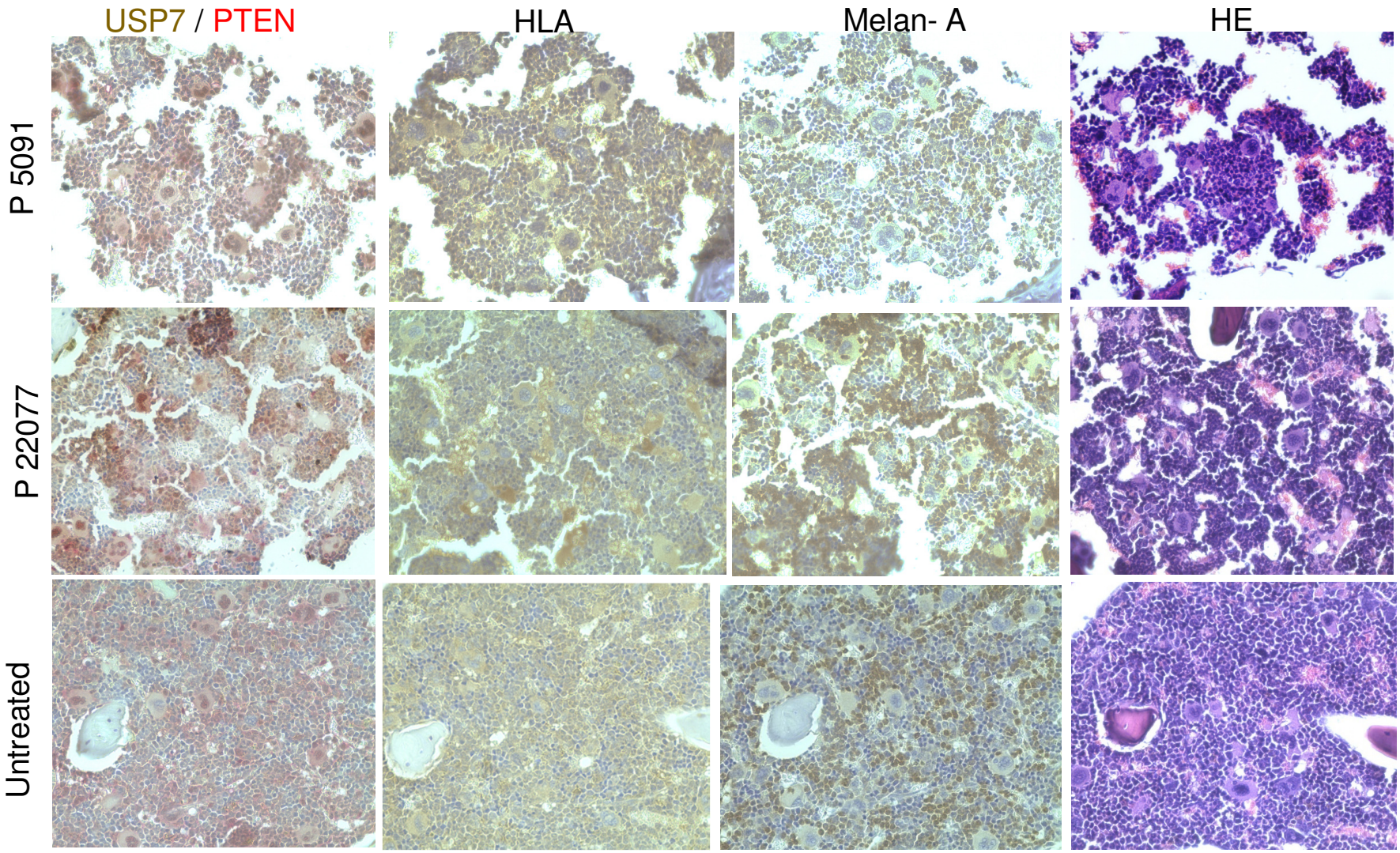

Extended figure S7b (i): Effect of USP7 inhibitors, P5091 and P22077 on metastatic potency of of BMRTCs population in CDXs. Histopathological evaluation of HLA, Mel-A, HE stain with co-localization USP7 and PTEN in similar BM region derived from USP7 inhibitor treated vs. untreated from CDXs (Patient #12). Scale bar=100 µm.

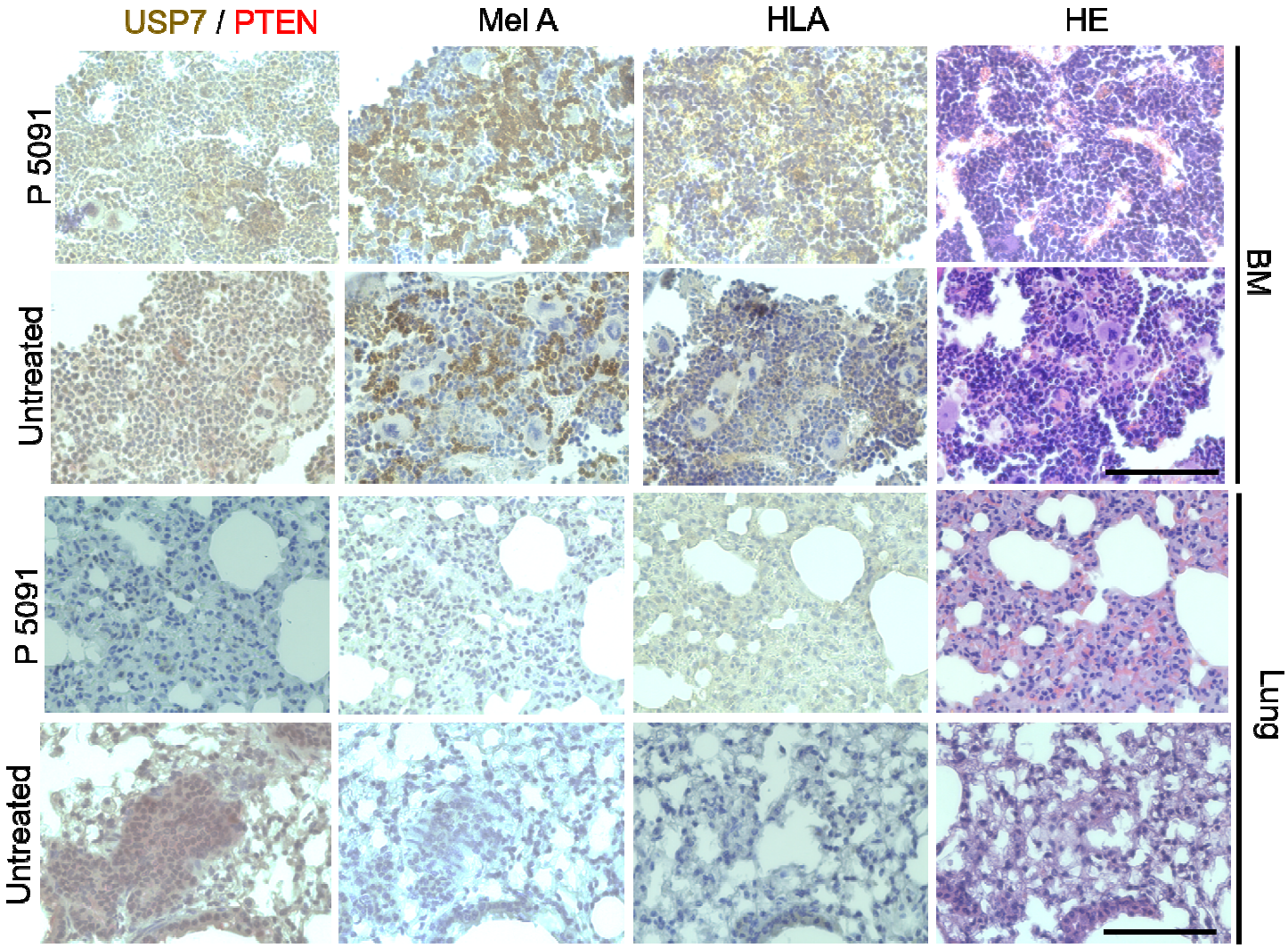

Extended figure S7b (ii): Effect of USP7 inhibitors, P5091 on metastatic potency of BMRTCs population in CDXs. Histopathological evaluation of HLA, Mel-A, HE stain with co-localization USP7 and PTEN in similar BM and lung region derived from USP7 inhibitor treated vs. untreated from CDXs (Patient #12). Scale bar=100 µm.

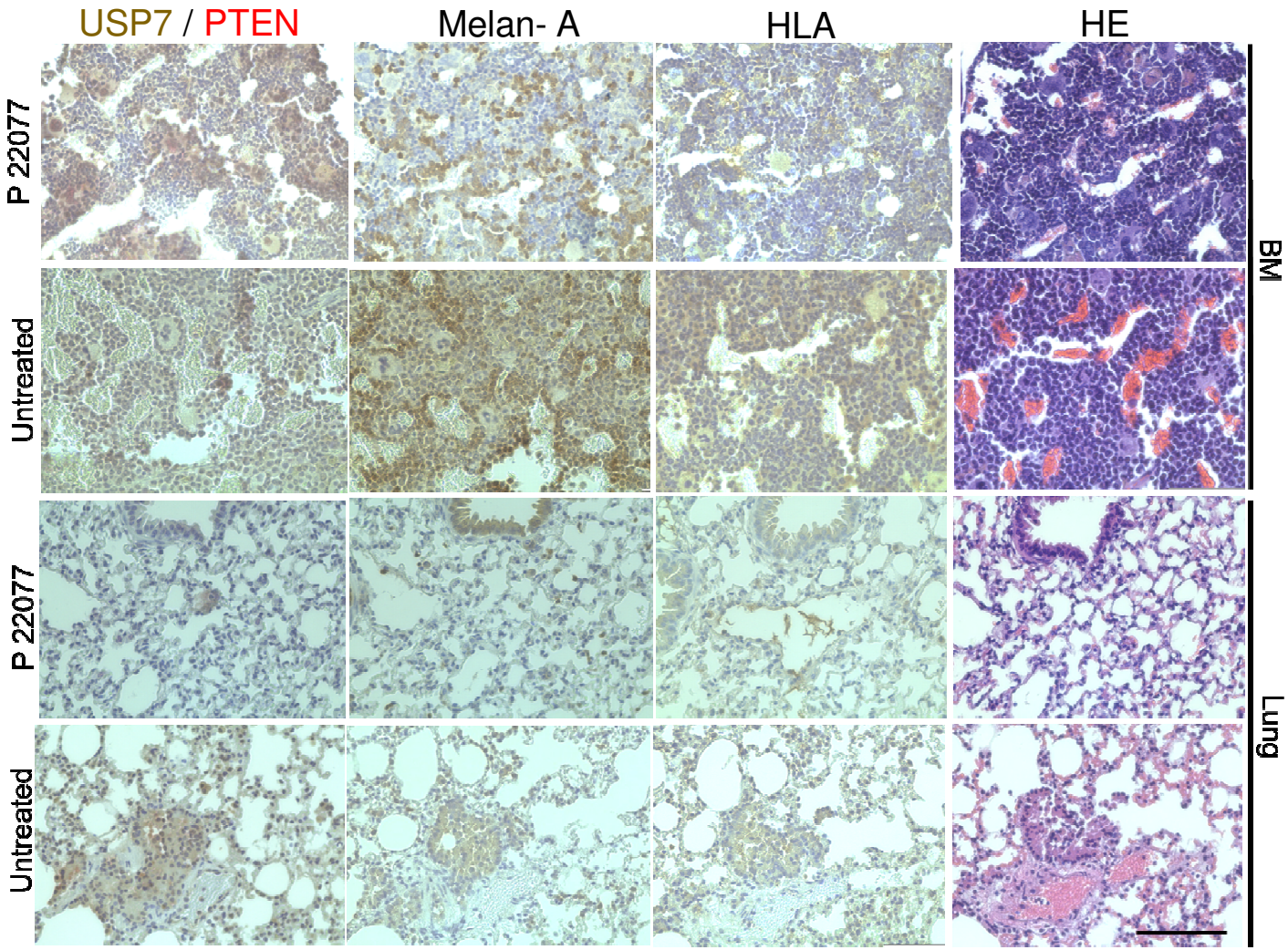

Extended figure S7c: Effect of USP7 inhibitors, P22077 on metastatic potency of of BMRTCs population in CDXs. Histopathological evaluation of HLA, Mel-A, HE stain with co-localization USP7 and PTEN in similar BM and lung region derived from USP7 inhibitor treated vs. untreated from CDXs (Patient #13). Scale bar=100 µm.

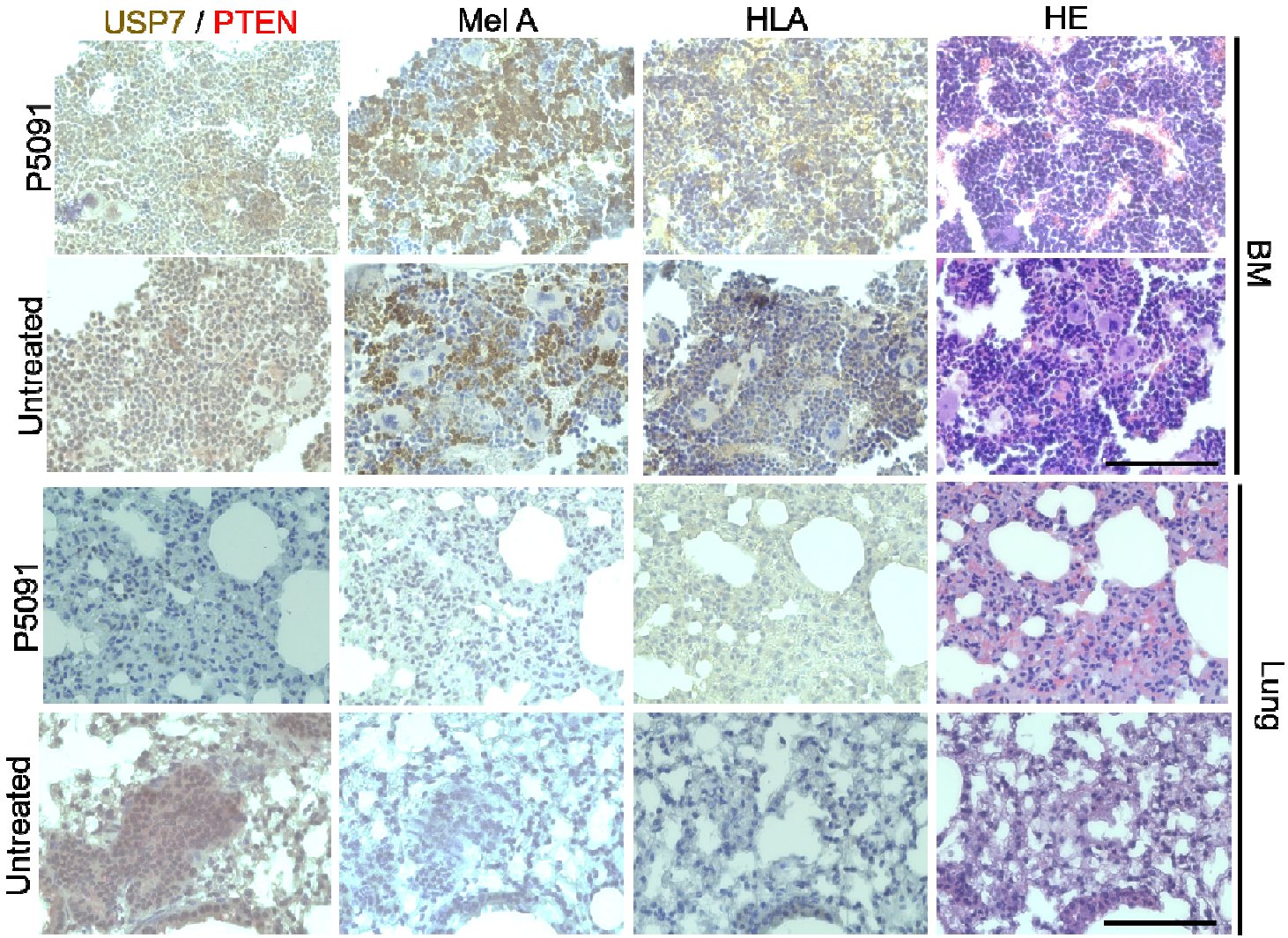

Extended figure S7d: Effect of USP7 inhibitors, P5091 on metastatic potency of of BMRTCs population in CDXs. Histopathological evaluation of HLA, Melan-A, HE stain with co-localization USP7 and PTEN in similar BM region derived from USP7 inhibitor treated vs. untreated from CDXs (Patient #14). Scale bar=100 µm.

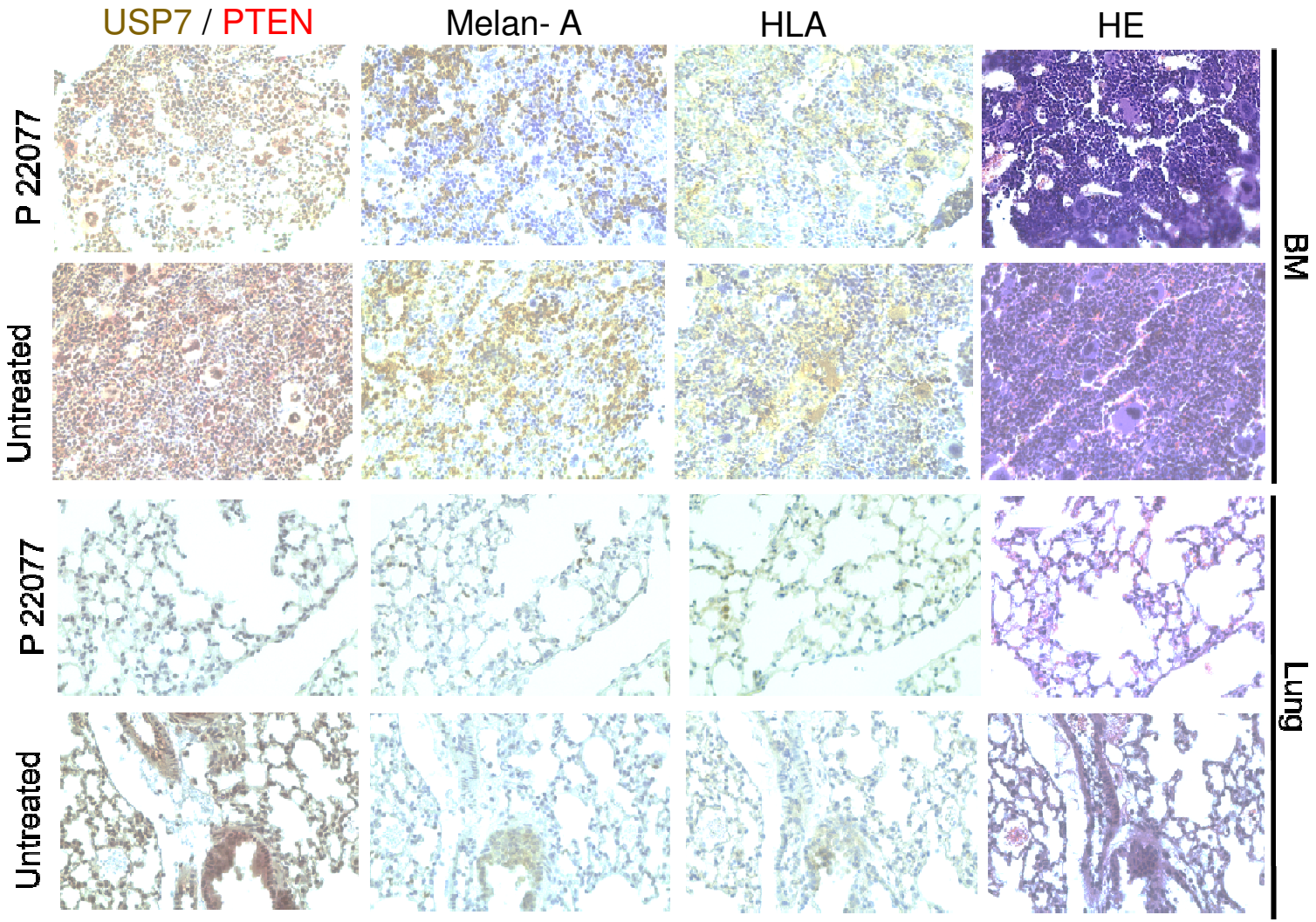

Extended figure S7e: Effect of USP7 inhibitors, P22077 on metastatic potency of of BMRTCs population in CDXs. Histopathological evaluation of HLA, Mel-A, HE stain with co-localization USP7 and PTEN in similar BM and lung region derived from USP7 inhibitor treated vs. untreated from CDXs (Patient #15). Scale bar=100 µm.

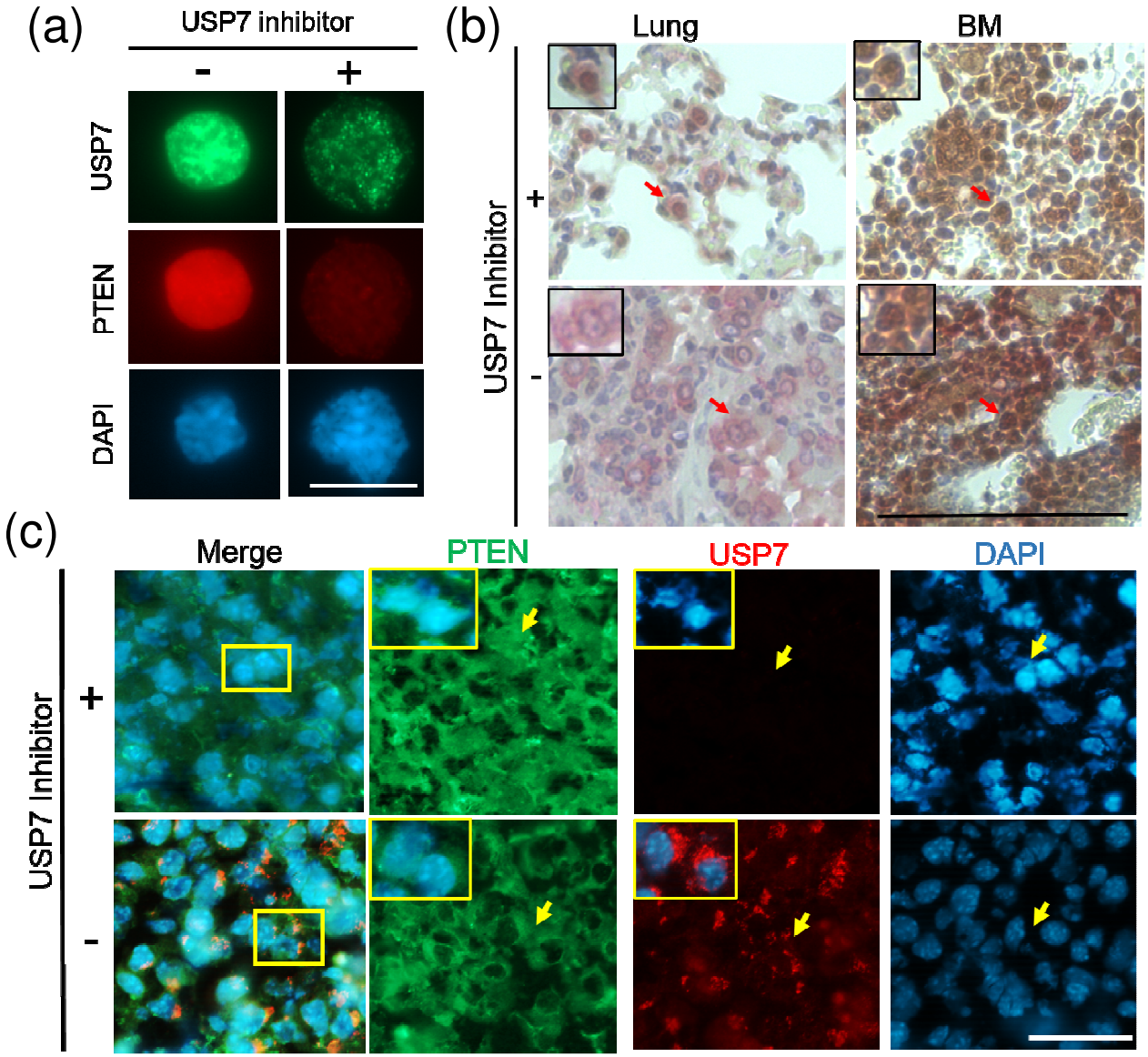

Supplementary figure S8 : Effect of USP7 inhibitors on localization of USP7 and PTEN expression (a) immunofluorescent analyses on flow-sorted HLA+ and Melan-A+ BMRTCs population derived from CDXs mice (scale bar=10 µM) (b) immunohistochemistry in lung and BM tissues (scale bar=100 µM) derived from CDXs mice. (c) immunofluorescent analyses in lung region of syngeneic mice (scale bar=50 µM); insets show bigger magnification of regions indicated by arrows.

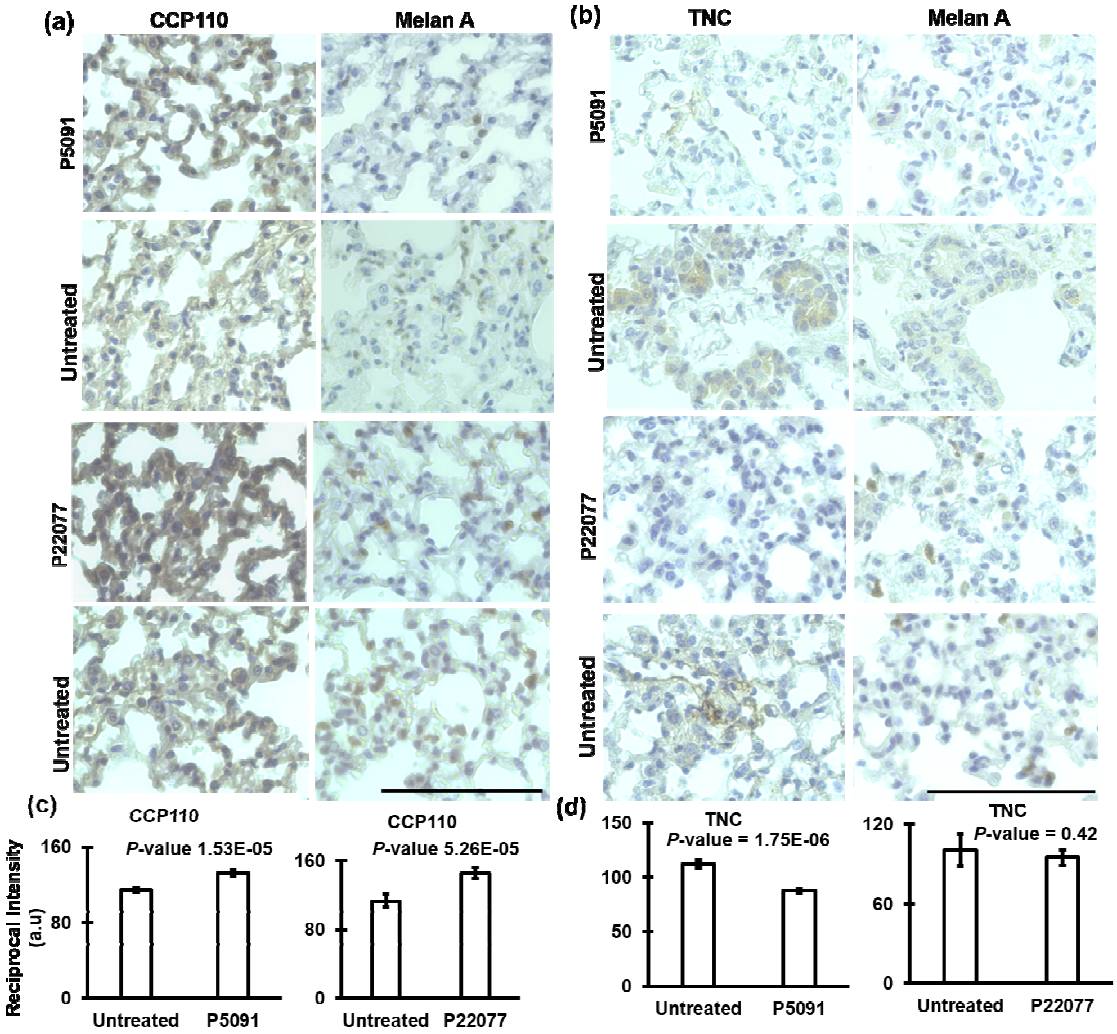

Supplementary figure S9: Effect of USP7 inhibitors (P5091 and P22077) in CDXS. Histopathological evaluation of CCP110 (Patient #11 and 16). TNC (Patients #11 and 15) and respective Melan-A staining in lung region derived from USP7 inhibitor treated vs untreated from CDXs. Scale bar=100 µm. Representative images are shown. Student t- test *paired 2, type 2,* was performed to calculate respective *P*-values.

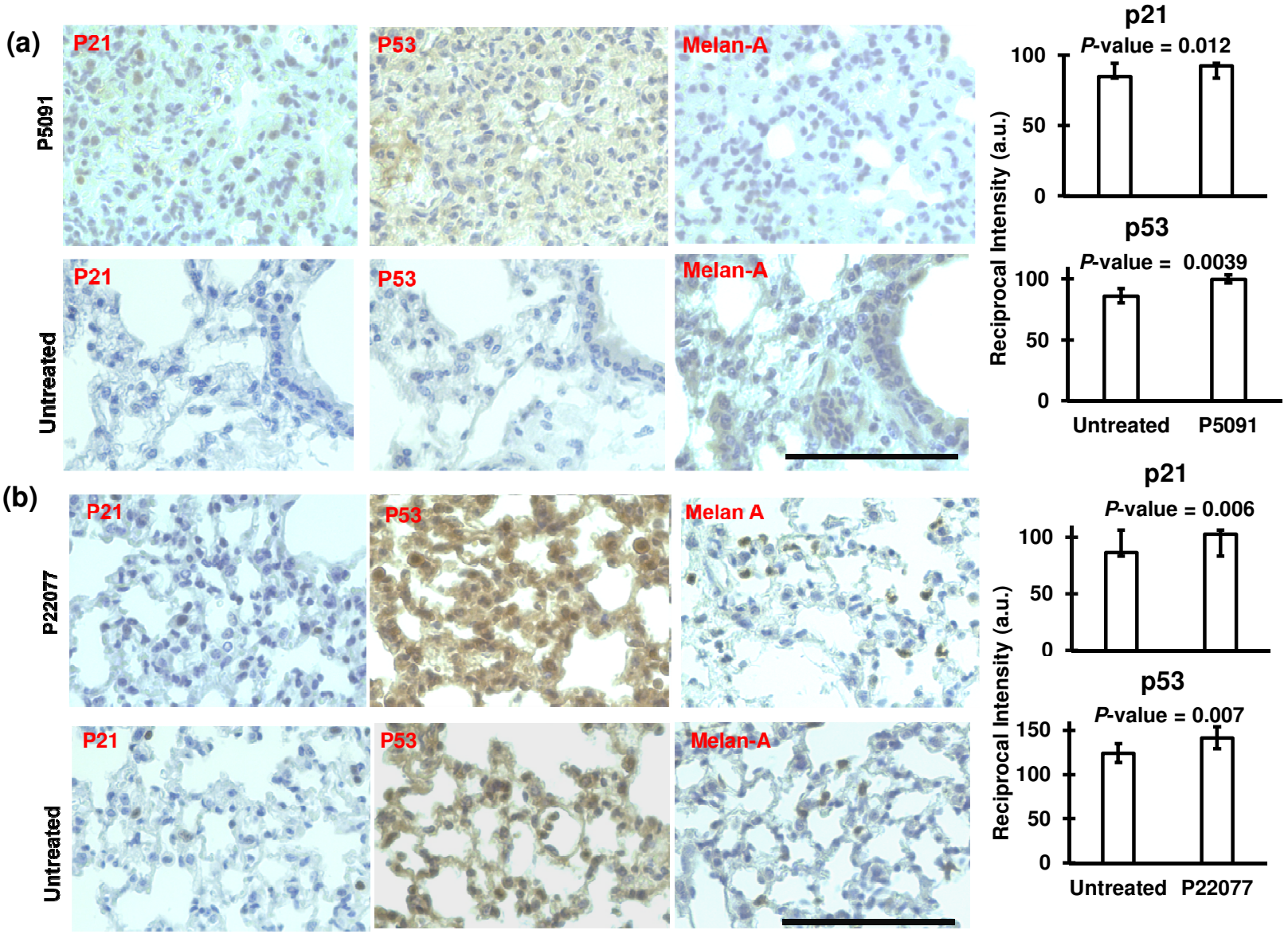

Supplementary figure S10 a & b: Effect of USP7 inhibitors [P5091 (a) and P22077 (b)] on P21/P53/Melan-A markers expression. Histopathological evaluation and signal intensity quantification of p21, p53 and Melan-A staining of same lung regions in USP7 inhibitor treated vs untreated from CDXs (Patient #13 and 15). Scale bar=100 µm. Representative images are shown. Student *t*-test *paired 2, type 2*, were performed to calculate respective *P*-value.

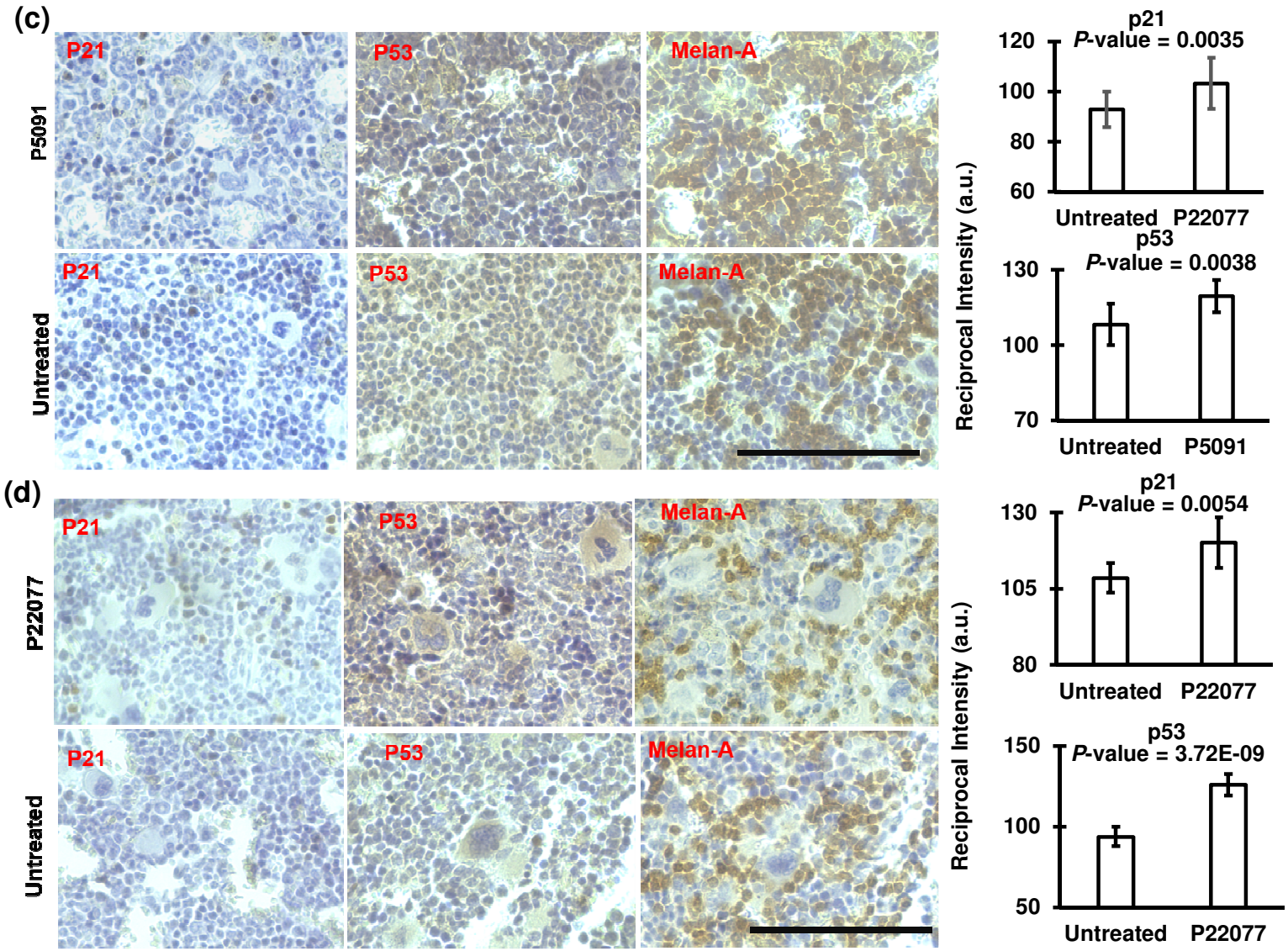

Supplementary figure S10 c & d: Effect of USP7 inhibitors [P5091 (c) and P22077 (d)] on P21/P53/Melan-A markers expression.

Histopathological evaluation and signal intensity quantification of p21, p53 and Melan-A staining of same BM regions in USP7 inhibitor treated vs untreated from CDXs (Patient# 13 and 15). Scale bar=100 µm. Student *t*- test *paired 2, type 2,* were performed to calculate respective *P*-values. Representative images are shown.

Supplementary table S1: Clinico-pathological parameters of advanced melanoma patients used for this study. Clinical parameters includes gender, age, site/type of primary tumor, tumor stage, mutational status, metastatic site with previous and current therapy of melanoma patients.

Patient ID	Gender	Age	Type of primary	Stage	Mutation Status	PTEN H- score	Site of disease at any time	Previous Therapies	Therapy at time of sample collectiom
1	Male	39	Cutaneous	IV M1c	BRAF V600E	NA	Brain (Leptomeninges only)	Dabrafenib, trametinib	Dabrafenib, trametinib
2	Male	49	unknown	IV M1c	BRAF V600K	75	Brain, lung, lymphnode, visceral, adrenal	Nivolumab, ipilimumab,dabrafenib, trametinib, pembrolizumab, abraxane	Pembrolizumab, abraxane
3	Male	72	Cutaneous	IV M1c	NRAS Q61R	72	Brain, soft tissue, subcutaneous, lymphnode	1038277	None
4	Male	74	Cutaneous	IV M1c	BCL9 G1373E, CDKN2A P114L, EGFR P733S, ERBB4 G286K, KNSTRN P28S, MYO18A V1342I, NF1 G1219R, R2450 (Nonsense), NRAS T50I, TET2 E350K, TP53 Q331 (Nonsense), Q317 (Nonsense), TSC1 P396S	60	Brain	None	None
5	Female	58	Acral lentiginous	IV M1c	BRAF V600E	250	Bone	None	None
6	Male	56	unknown	IV M1a	BRAF V600E, Tp53	25	Lymphnode	Ipilimumab	Pembrolizumab
7	Male	27	Cutaneous	IIIB	NRAS Q61k, CDNK2A E61	NA	Lymphnode	None	None
8	Male	69	unknown	IV M1c	BRAF negative	NA	Liver, lung	None	Ipilimumab, nivolumab
9	Female	65	Cutaneous	IV M1b	BRAF V600E, ERBB2 V773M	NA	Lymphnode, (Leptomeninges)	Nivolumab	Nivolumab
10	Female	67	Cutaneous	IV M1c	BRAF V600E, CDKN2A R124 (Frameshift)18, ATM V2705I	NA	Brain, soft tissue, visceral	None	Dabrafenib, trametinib
11	Male	75	Cutaneous	IV M1c	PDGFRA D846N	70	Brain, lung	None	None
12	Male	67	Cutaneous	IV M1b	Unknown	280	Skin, lung	None	None
13	Female	37	Cutaneous	IV M1c	BRAF V600E	0	Brain, lungs, liver, bone, spleen, soft tissue	Dabrafenib,trametinib, pembrolizumab	Pembrolizumab, dabrafenib, trametinib
14	Female	58	Cutaneous	IV M1c	BRAF V600E	280	Brain, skin, lymphnode, lung	Ipilimumab, dabrafenib, trametinib	Pembrolizumab
15	Male	52	Cutaneous	IIIB	Unknown	300	lymphnode	None	None
16	Female	55	unknown	IV M1c	CDKN2A R80 (Nonsense), CDKN2A A68 frameshift78,FGFR3 G784E	NA	Brain	None	Ipilimumab, nivolumab

Supplementary table S2: Downregulated proliferative markers analyzed by microarray in patient-derived Lin-neg vs. healthy donor PBMCs population

Gene Symbol	Fold Change	*P*-value
PCNA	-24	9.01E-07
MKI67	-3.02	0.0075
RBL2	-379.96	3.73E-11
CDK6	-11.52	1.13E-05
CDKN1A	-6.62	0.0303
CDKN1B	-12.75	4.10E-05
DEK	-36.39	8.33E-06
DDX39A	-23.05	2.26E-05
CCNB1	-2.61	0.0006
SGOL1	-4.41	3.39E-05
RRM2	-7.16	0.0001
TOP2A	-4.91	0.0003
H2AFZ	-9.15	1.49E-05
HAT1	-310.55	1.33E-09
CAPZA1	-137.54	6.40E-10
HADHB	-51	1.03E-08
IDH3A	-68.9	2.83E-09
KPNA2	-24.31	2.65E-07
PGK1	-221.21	6.74E-08

Supplementary table S3: Upregulated melanoma markers analyzed by microarray in patient-derived Lin-neg vs. healthy donor PBMCs population

Gene Symbol	Fold Change	*P*-value
DEC1	2.75	9.14E-06
B4GALNT1	2.74	0.0001
BAGE; BAGE4; BAGE3; BAGE2; BAGE5	3.24	4.28E-06
MAGEA1	4.06	4.25E-05
DCD	2.61	0.0045
S100A3	2.78	0.0005
S100A7L2	2.99	0.0093
S100P	6.67	0.0006

Supplementary table S4: Gene primers sequence used in this study

Gene	Forward Primer 5'-3'	Reverse Primer 5'-3'
USP7	GACCGATCCTGAGAAAGGATTTAT	CGTAGCCTGTGTGCTTCTT
PTEN	TGGATTCGACTTAGACTTGACCT	GGTGGGTTATGGTCTTCAAAAGG
Tenascin-C	CGAGAAAGGCAGACACAAGA	GATGGAGACTGTATAAGGCGTAG
RGS22	TGGATCACAGTGGAATGAAGAG	CAAGAGGGTTGCCATTTGTG
GPCPD1	GAGTTCAAGTGCAGGCATTC	GAGACAAGCTGTACCCACAT

***Please note*: Supplementary table S5 containing genomic mutational analysis of Lin-neg/CTC enriched population derived from CDX models (S5a and S5b) are provided in supplementary excel files.**

Supplementary table S6: Tables showing top five significantly altered canonical pathways in Lin-neg cell population by Ingenuity pathway analyses.

	Ingenuity Canonical Pathways	-log(p-value)	Ratio	z-score	# of Molecules
Activated	RhoGDI Signaling	5.62E-03	0.393	5.939	7
	PTEN Signaling	5.87E-06	0.496	4.276	14
	PPAR Signaling	1.44E-02	0.411	4.003	7
	Role of p14/p19ARF in Tumor Suppression	1.11E-03	0.535	3.838	2
	PPARα/RXRα Activation	5.51E-05	0.439	3.3	22
Inhibited	Role of NFAT in Regulation of the Immune Response	1.67E-15	0.581	-9.077	90
	IL-8 Signaling	3.37E-05	0.437	-9.055	87
	Phospholipase C Signaling	1.78E-08	0.471	-9.037	94
	NF-κB Signaling	1.40E-09	0.514	-8.91	99
	Integrin Signaling	3.43E-09	0.489	-8.889	9

Supplementary table S7: Tables showing cellular functions in Lin-neg cell population by Ingenuity pathway analyses.

	Functions Annotation	*p*-Value	Activation z-score	# of Molecules
Activated	organismal death	4.15E-26	32.077	1343
	morbidity or mortality	2.21E-26	31.785	1360
	Growth Failure	2.2E-10	17.474	334
	hypoplasia of lymphatic system	1.38E-13	10.023	105
	hypoplasia of lymphoid organ	4.32E-13	9.83	101
Inhibited	infection by RNA virus	4.9E-46	-19.961	620
	infection by Retroviridae	2.02E-40	-19.699	503
	HIV infection	2.21E-40	-19.675	499
	infection of cells	1.64E-52	-19.587	562
	infection by lentivirus	1.07E-40	-19.568	501

Supplementary table S8: Specific mutations in BMRTCs (HLA+/MelA+ cell population of xenografts)

Chrom	Position	Ref	Variant	Allele Call	Gene ID
chr18	48575100	C	G	Homozygous	SMAD4
chr18	48575118	T	A	Homozygous	SMAD4
chr18	48575124	A	G	Homozygous	SMAD4
chr18	48575136	A	G	Homozygous	SMAD4
chr18	48575178	T	C	Homozygous	SMAD4
chr18	48575205	C	T	Homozygous	SMAD4
chr18	48575208	A	G	Homozygous	SMAD4
chr18	48575211	A	G	Homozygous	SMAD4
chr5	112175578	A	G	Homozygous	APC
chr5	112175599	T	C	Homozygous	APC
chr5	112175605	A	C	Heterozygous	APC
chr5	112175608	T	C	Heterozygous	APC
chr5	112175614	A	T	Heterozygous	APC
chr5	112175755	A	G	Homozygous	APC
chr5	112175761	TTTT	CTTC	Homozygous	APC
chr5	112175992	A	T	Homozygous	APC
chr5	112176014	C	T	Homozygous	APC
chr5	112176034	T	A	Heterozygous	APC

Supplementary table S9: Top five upstream regulators and their functional annotation in BMRTCs vs CTCs populations derived from melanoma patient-derived CDXs models (Patients #1-8)

	Upstream Regulator	Molecule Type	Activation *z*-score	*p*-value	# of Molecules	Diseases or Functions Annotation	*p*-Value	Activation *z*-score	# Molecules
Activated	NFE2L2	transcription regulator	5.617	0.0175	34	Viral Infection	2.08E-14	11.435	217
	ESR1	ligand-dependent nuclear receptor	5.258	0.000149	105	infection by RNA virus	4.35E-15	10.698	142
	1,2-dithiol-3-thione	chemical reagent	5.073	0.000137	26	infection of cells	1.7E-17	10.448	133
	TGFB1	growth factor	4.727	0.00729	123	infection by HIV-1	3.87E-14	9.979	103
	XBP1	transcription regulator	4.621	0.00025	25	HIV infection	3.82E-11	9.794	109
Inhibited	CD 437	chemical drug	-5.667	1.38E-09	36	organismal death	4.52E-12	-14.901	293
	ST1926	chemical drug	-5.468	9.05E-09	30	morbidity or mortality	7.74E-12	-14.827	295
	miR-16-5p	mature microrna	-5.33	5.47E-06	29	Growth Failure	8.09E-05	-8.334	74
	RICTOR	other	-5.145	7.33E-06	34	death of embryo	5.5E-10	-5.699	33
	CD3	complex	-4.972	0.00133	55	anemia	4.52E-05	-4.917	54